OL Organic Letters

pubs.acs.org/OrgLett

Letter

Butterfly-Shaped Dibenz[*a*,*j*]anthracenes: Synthesis and Photophysical Properties

Yan-Ying Wu, Yi-Lin Wu,* Cheng-Lan Lin,* Hung-Cheng Chen, Yao-Yuan Chuang, Chih-Hsien Chen,* and Chih-Ming Chou*

Cite This: https://doi.org/10.1021/acs.orglett.3c02306

Read Online

ACCESS | Metrics & More | Article Recommendations | Supporting Information

ABSTRACT: A strategy for the synthesis of dibenz[*a*,*j*]-anthracenes (DBAs) from cyclohexa-2,5-diene-1-carboxylic acids is presented. Our approach involves sequential C−H olefination, cycloaddition, and decarboxylative aromatization. In the key step for DBA skeleton construction, the bis-C−H olefination products, 1,3-dienes, are utilized as substrates for [4 + 2] cycloaddition with benzyne. This concise synthetic route allows for regioselective ring formation and functional group introduction. The structural features and photophysical properties of the resulting DBA molecules are discussed.

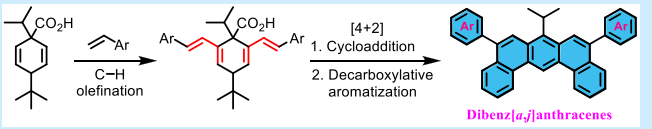

The quest for new synthetic strategies for polycyclic aromatic hydrocarbons (PAHs) has been motivated by the rich chemistry that they have exhibited over the past 50 years. PAHs, known for their π-conjugated electronic structure, have long been a testing ground for theoretical developments concerning aromaticity, open-shell radicals, and quantum chemical calculations.[1] These π-extended aromatic molecules possess a low energy gap between the frontier orbitals, particularly in the ultraviolet−visible−near-infrared (UV−vis−NIR) region, and feature accessible redox chemistry and noncovalent interactions. Consequently, PAHs have emerged as highly promising materials for diverse applications in optoelectronics, sensing, and energy conversion.[2]

While linearly ring-fused PAHs (acenes) exhibit intriguing potential for applications such as field-effect transistors and singlet exciton fission,[3] their practical utilization has been impeded by their inherent instability. Substantial efforts have thus been directed toward exploring two-dimensional or angularly fused PAHs.[4] A notable example is the class of angularly fused bis(tetracene) derivatives. These compounds were found to exhibit enhanced stability under ambient conditions and successfully employed as air-stable organic semiconductors in field-effect transistors and organic photovoltaics.[5] Additionally, helicenes, featuring *ortho*-fused aromatic rings, display interesting electronic and optical properties, including circularly polarized luminescence and electron spin filter behavior, as a result of their structural chirality.[6] These advancements have been achieved in conjunction with the pursuit of structurally and topologically precise subunits of graphene,[7] enabling precise control over their electronic and optical properties, and have fueled enthusiasm for the development of novel PAH-based materials.

In this context, dibenz[*a*,*j*]anthracene (DBA; Scheme 1) can be considered a particularly interesting PAH as a result of the combination of linearly and angularly fused ring architecture. This underdeveloped class of PAHs has been utilized to build *J*-aggregating emissive macrocycles[8] and rigid molecular receptors,[9] has served as a precursor to construct the zigzag edge of topologically specific graphitic nanoribbons,[10] and can be regarded as a building block for coronoid hydrocarbons.[11] The early approach to construct such aromatic systems involved photocyclization[12] or Diels−Alder reaction[13] (Scheme 1a); however, these methods often result in a mixture of regioisomers. More recently, ring-closing metathesis[14] and electrophilic cyclization[10a,15] from olefinic and acetylenic precursors, respectively, have been explored to achieve better control over product geometry. The elaborated precursors used in these methods limit the introduction of functionalities to DBA, and in some cases, specific sites of the starting materials need to be blocked to ensure regiospecificity.

Building upon our recently developed protocols for C(alkenyl)−H functionalizations of cyclohexa-2,5-diene-1-carboxylic acids (**A**; Scheme 1b),[16] we envisioned that constructing the angularly fused ring skeleton from this bilateral 1,3-diene would prescribe the Diels−Alder reaction with a high level of regiochemical control. The Pd-coordinative carboxylic acid functionality (a "transient directing group") could aid in introducing desired functionalities and enable decarboxylative aromatization of proaromatic compound **B**, ultimately yielding DBA. In light of this possibility, we present here a regiospecific DBA synthesis through tandem Pd-catalyzed directed C−H olefination, Diels−Alder cyclization,

Received: July 16, 2023

Scheme 1. Synthetic Strategies for DBA

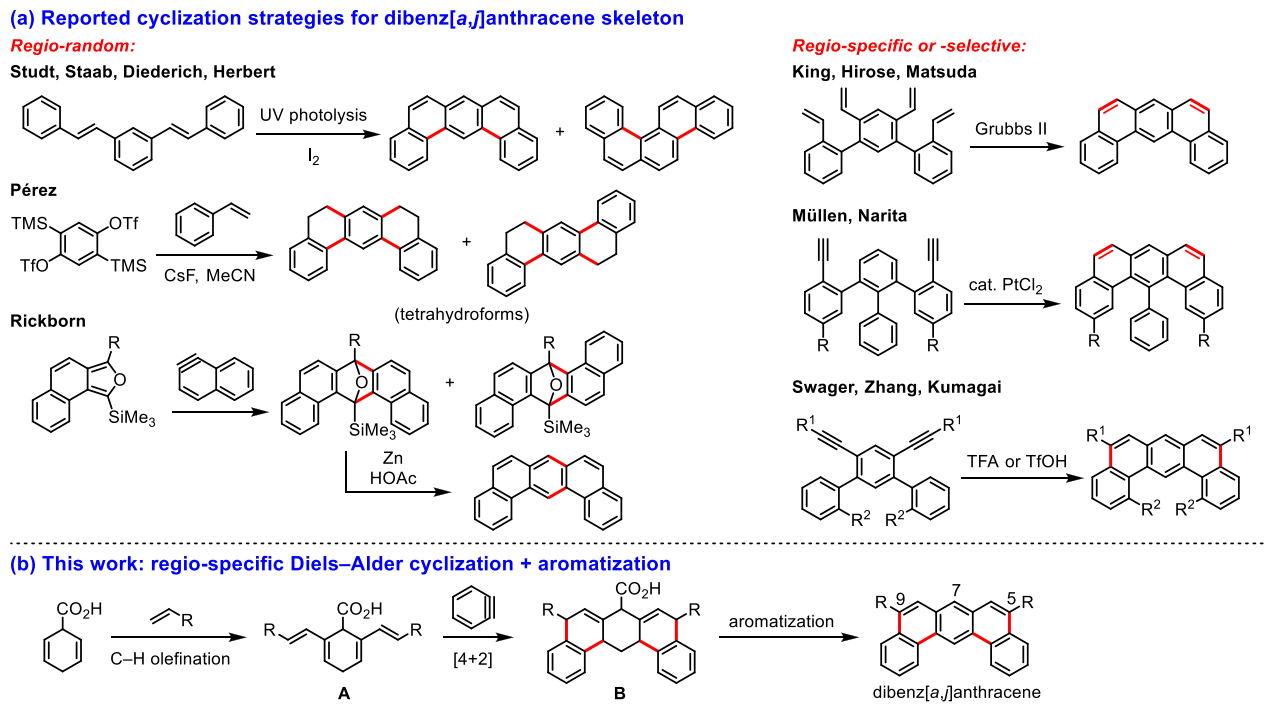

Scheme 2. Synthetic Route for Diaryl Dibenzanthracenes and Diaryl Dinaphthoanthracene

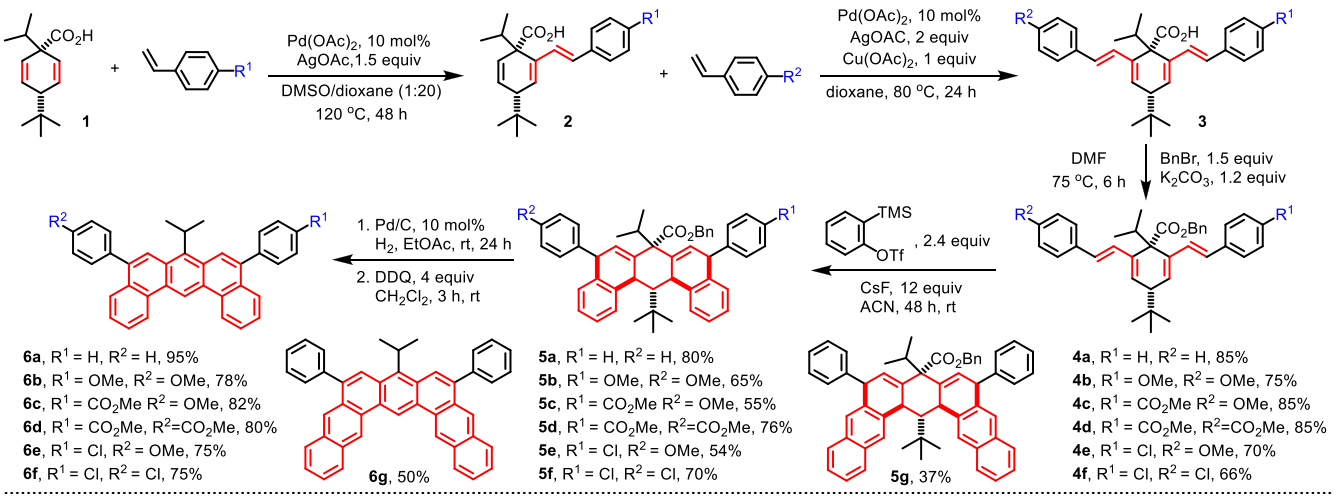

and oxidative aromatization. This method enables the introduction of functional groups at positions 5 and 9, and the size of angularly fused PAH can be varied by selecting the appropriate aryne precursor for the Diels–Alder reaction. Furthermore, we discuss the mechanism of formation, structural properties, UV–vis absorption and emission, and electrochemical properties of these DBA derivatives.

The synthesis of 5,9-disubstituted DBA commenced with a sequential carboxylate-directed Pd-catalyzed C(alkenyl)–H olefination of 4-(*t*-butyl)-1-*i*-propylcyclohexa-2,5-diene-1-carboxylic acid (**1**; Scheme 2). The *t*-butyl group of the starting material reduces the tendency of competing decarboxylative aromatization in the stage of olefination to give compounds **2** and **3**. Thus, the sequential olefination can occur under a similar condition to afford symmetric and asymmetric bilateral 1,3-diene **3** using our Pd-catalyzed C–H activation protocols in good yields over two steps.[16b] After esterification with benzyl bromide, bis(butadiene) **4** was then treated with *in situ* generated benzyne or 2-naphthyne to give proaromatic intermediate **5** in 37–80% yields. The electronic characteristics of the butadiene moiety show little bearing on the outcome of the Diels–Alder reaction of compound **4**. On the other hand, the low thermal stability of naphthyne may contribute to the low yield for compound **5g**. After deprotection of the benzyl group, in the final stage of the synthesis, 2,3-dichloro-5,6-dicyano-1,4-benzoquinone (DDQ) was exploited to achieve decarboxylative (the central ring) and oxidative (the "angled" rings) aromatization of compound **5** to give the DBA ring system (**6**) in 50–95%. The structural determination of compound **6** was supported by ^{1}H and ^{13}C nuclear magnetic resonance (NMR) spectroscopy, high-resolution mass spec-

https://doi.org/10.1021/acs.orglett.3c02306
Org. Lett. XXXX, XXX, XXX–XXX

trometry, and single-crystal X-ray diffraction (see the later discussion).

Although bilateral 1,3-diene **3** can be, in principle, a suitable substrate for Diels–Alder reaction with aryne, we have reported that its carboxylic acid functionality would also react with aryne to give aryl ester (along with other side reactions).[16b,17] To avoid the undesirable consumption of valuable aryne precursors, it was decided to convert compound **3** into benzyl ester **4**. The desired carboxylic acid functionality could later be liberated by hydrogenation prior to oxidative aromatization. Methyl esters had been considered an alternative to benzyl esters **4**; however, hydrolysis of the methyl ester analogue of compound **5a** was unsuccessful (compound **5aa**; see the Supporting Information).

It is unanticipated that we observed the elimination of the *t*-butyl group instead of a simple hydride in the final oxidative aromatization of compound **5**. Such a process is likely to occur through the mechanism shown in Scheme 3. In the first two steps i and ii, dehydrogenative oxidation in the "angled" rings proceeds through the sequential removal of hydride and protons by DDQ.[18] Finally, hydride transfer from the *t*-butyl group to (protonated) quinone is then driven by the elimination of CO_2 and isobutene and the relief of steric congestion around the *t*-butyl group to give aromatized dibenz[*a*,*j*]anthracenes.

Scheme 3. Proposed Mechanism for Oxidative and Decarboxylative Aromatization by DDQ

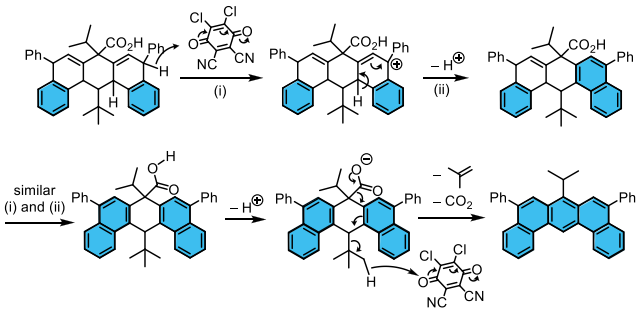

The structure of DBA **6a** is confirmed by single-crystal X-ray diffraction analysis, which shows five consecutive fused rings in a nearly planar geometry (Figure 1). To the best of our knowledge, this is the first DBA crystal structure without substituents in the "gulf" region (14 position).[15b,19] Edge-to-face C–H···π (C···C = 3.55 Å between the Ph substituent and the terminal benzo ring) and π···π (3.72 Å between the mean planes of neighboring molecules) contacts are likely responsible for the observed dimer pairs in the solid. A slight nonplanarity of 17° between the two planes defined by two terminal benzene units of DBA was observed. We believe such a torsion results from the asymmetric intermolecular packing features described above but not intrinsic to the DBA skeleton, supported by the planar geometry found in the density functional theory (DFT)-optimized structure at the level of ωB97X-D/6-31G(d,p) (Gaussian 09; see the Supporting Information for the full citation). No extended π stack was found, which is consistent with the excellent solubility of compound **6** in common organic solvents. As anticipated, the "angled" rings in compound **6a** display noticeable C–C/C=C bond length alternation and are less aromatic; the C_5–C_6 and C_8–C_9 bonds are about 1.36 Å, typical of a formally C=C double bond ("d" bonds in Figure 1a), whereas three other bonds in these rings are about 1.45 Å ("s" bonds), in accordance with Clar's aromatic sextet rule.[20]

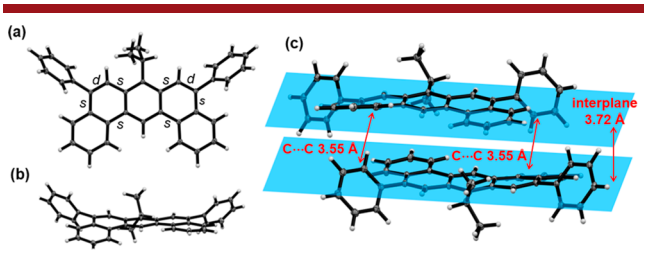

Figure 1. X-ray crystal structure of compound **6a** (thermal ellipsoids are shown at 50% probability): (a) top view of compound **6a**, (b) side view of compound **6a** highlighting the non-planarity, and (c) close edge-to-face C–H···π and π···π contacts between neighboring molecules. C–C bond distances are in the range of 1.44–1.46 Å for the s type and 1.36 Å for the d type.

These nonlinear DBAs are colorless in solutions, unlike purple-colored pentacene (absorption λ_{max} ~ 600 nm in solutions), an isomeric PAH with five linearly fused benzene rings. Variations of the electronic nature of the substituents on the 5- and 9-phenyl substituents of DBA **6a–6f** caused a negligible effect on their photophysical properties (Table 1).

Table 1. Optical and Electrochemical Properties of Compounds 6a–6g

	λ_{max}[a] (nm) [ε (M^{-1} cm^{-1})]	Φ_{PL}[b] (%)	λ_{em}[a] (nm)	$E_{ox,onset}$[c] (V)
6a	315 [22000]	7.80	420, 440	0.96
6b	318 [33000]	9.10	421, 442	0.82
6c	322 [30000]	11.50	426, 446	0.78
6d	319 [32000]	9.50	424, 444	0.89
6e	317 [28000]	9.30	423, 442	0.75
6f	316 [33000]	5.30	421, 439	0.85
6g	350 [35000]	6.50	451, 479	0.83

[a]Measured in EtOAc. [b]Absolute photoluminescence quantum efficiency, measured using an integrating sphere. [c]Measured in a CH_2Cl_2 solution containing 0.1 M nBu_4NClO_4 (V versus Ag/Ag^+).

The onsets of UV absorption are around 380 nm with the absorption maxima λ_{max} ~ 320 nm measured in ethyl acetate, and blue emissions were found in λ_{em} of 420–426 nm for compounds **6a–6f** (Figure 2). Naphtho-fused compound **6g**, on the other hand, shows a noticeable red shift in absorption

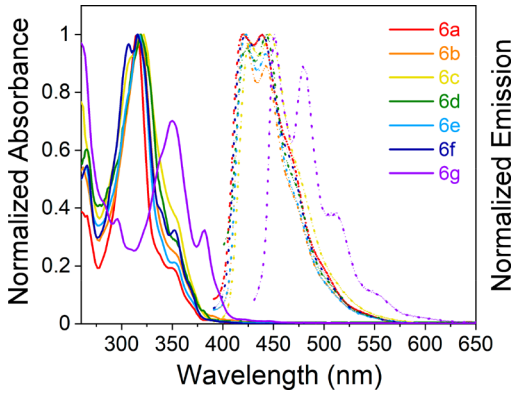

Figure 2. Normalized absorption (solid lines) and emission (dashed lines) of compounds **6a–6g** were recorded in ethyl acetate.

https://doi.org/10.1021/acs.orglett.3c02306
Org. Lett. XXXX, XXX, XXX–XXX

and emission with its large π-conjugated aromatic core. It should be noted that the apparent large Stoke shift between λ_{max} and λ_{em} is due to the very weak $S_0 \rightarrow S_1$ transition (around the absorption onset at 380 nm) compared to the higher energy transitions. While $S_0 \rightarrow S_2$ has a dominating highest occupied molecular orbital (HOMO) → least unoccupied molecular orbital (LUMO) character (DFT-computed oscillator strength f of 0.02−0.03; Table S1 of the Supporting Information), $S_0 \rightarrow S_1$ and $S_0 \rightarrow S_3$ feature anti- and in-phase configuration interactions of HOMO − 1 → LUMO and HOMO → LUMO + 1, respectively, resulting in nearly forbidden S_1 ($f \sim 0.000-0.005$) but strong S_3 ($f \sim 1.37-2.35$) transitions, commonly observed for alternant aromatic hydrocarbons of small-to-medium size.[21] Although electron donor−acceptor substitution (e.g., compounds **6c** and **6e**) allows for some mixing of the three transition configurations mentioned above (see section 6 of the Supporting Information), it was not found to be sufficient to alter the nature of the S_1 state and increase its oscillator strength. Despite the "dark" nature of S_1, these molecules show highly structured emission profiles with moderate photoluminescence quantum yields (Φ_{PL} of 5−12%), corroborating a rigid molecular structure to avoid nonradiative vibrational relaxation.

The insensitivity of the optical transition energy to the nature of 5,9 substituents of compounds **6a**−**6f** is usually considered evidence of the parallel shifting of the HOMO and LUMO energy. The cyclic voltammograms of the compounds are depicted in Figure S1 of the Supporting Information. The onset potential of the electrochemical oxidation, $E_{ox,onset}$, was estimated and is listed in Table 1. The oxidation reactions were found to be irreversible. The absence of cathodic current responses with a magnitude comparable to that of the anodic current responses raises uncertainty regarding the reliable estimation of the LUMO of the compounds. Furthermore, the estimation of the LUMO level by optical absorption is complicated by the non-HOMO-to-LUMO character of the S_1 state. However, we note that the invariance in the excitation energy for compounds **6a**−**6f** is well-reproduced by time-dependent density functional theory (TD-DFT) calculations (Table S1 of the Supporting Information). Additionally, a good correlation was found between the computed HOMO and LUMO energy with the average Hammett substituent constants σ_p, instead of the Hammett constant of the more electron-rich (for HOMO) or electron-poor (for LUMO) substituent (Figures S2 and S3 of the Supporting Information). Such a correlation indicates that the substituents on the 5,9-diphenyl groups in compounds **6a**−**6f** only influence the electron structure of DBA in a perturbative way but do not dominate the overall properties of the molecule. This observation is in line with the leading contribution of the DBA core motif to the molecular frontier orbitals in comparison to that of the 5,9-diphenyl groups (Figure 3).

In conclusion, the developed synthetic approach enables the regiospecific synthesis of DBA derivatives with controlled functionalization. The key step of the synthesis involves the Diels−Alder reaction with proaromatic butadiene precursors, while the subsequent oxidation exhibits an unusual elimination of the *t*-butyl group during decarboxylative aromatization. Although the 5,9-diphenyl substituents do not have a significant impact on the optical properties of the synthesized compounds, our analysis provided valuable insights into this observation. Building upon these findings, our ongoing research aims to explore the full potential of the DBA scaffold by introducing heterocycles and five-membered ring motifs. This exploration seeks to enhance the optical absorption properties of DBA derivatives in terms of visible-light absorptivity and emission intensity.

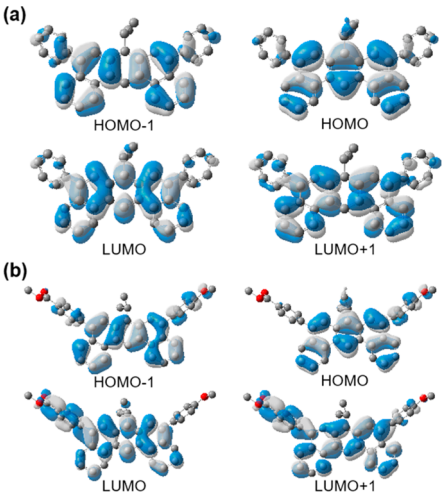

Figure 3. Visualization of frontier orbitals of compounds (a) **6a** and (b) **6c**, representative of symmetrically and asymmetrically substituted DBAs, respectively.

■ ASSOCIATED CONTENT

Data Availability Statement

The data underlying this study are available in the published article and its Supporting Information.

Supporting Information

The Supporting Information is available free of charge at https://pubs.acs.org/doi/10.1021/acs.orglett.3c02306.

Experimental procedures, characterization data, NMR spectra, crystallographic data, and electrochemical and DFT analyses (PDF)

Accession Codes

CCDC 2181649 contains the supplementary crystallographic data for this paper. These data can be obtained free of charge via www.ccdc.cam.ac.uk/data_request/cif, or by emailing data_request@ccdc.cam.ac.uk, or by contacting The Cambridge Crystallographic Data Centre, 12 Union Road, Cambridge CB2 1EZ, UK; fax: +44 1223 336033.

■ AUTHOR INFORMATION

Corresponding Authors

Chih-Ming Chou − *Department of Applied Chemistry, National University of Kaohsiung, Kaohsiung 81148, Taiwan*; Email: cmchou@nuk.edu.tw

Yi-Lin Wu − *School of Chemistry, Cardiff University, Cardiff CF10 3AT, United Kingdom*; Email: WuYL@cardiff.ac.uk

Cheng-Lan Lin − *Department of Chemical and Materials Engineering, Tamkang University, New Taipei City 251301, Taiwan*; Email: cllin@mail.tku.edu.tw

Chih-Hsien Chen − *Department of Chemical Engineering, Feng Chia University, Taichung 407, Taiwan*; Email: chschen@fcu.edu.tw

Authors

Yan-Ying Wu − *Department of Applied Chemistry, National University of Kaohsiung, Kaohsiung 81148, Taiwan*

https://doi.org/10.1021/acs.orglett.3c02306
Org. Lett. XXXX, XXX, XXX−XXX

Hung-Cheng Chen − *Department of Applied Chemistry, National University of Kaohsiung, Kaohsiung 81148, Taiwan*
Yao-Yuan Chuang − *Department of Applied Chemistry, National University of Kaohsiung, Kaohsiung 81148, Taiwan*

Complete contact information is available at: https://pubs.acs.org/10.1021/acs.orglett.3c02306

Notes

The authors declare no competing financial interest.

■ ACKNOWLEDGMENTS

The authors gratefully thank the National University of Kaohsiung and the Ministry of Science and Technology of Taiwan (MOST 110-2628-M-390-001-MY4) for their financial support. The Core Facility Center at the National Cheng Kung University (HRMS and X-ray crystallography) is acknowledged. Part of this research was undertaken using the supercomputing facilities at Cardiff University operated by Advanced Research Computing at Cardiff (ARCCA) on behalf of the Cardiff Supercomputing Facility and the HPC Wales and Supercomputing Wales (SCW) projects. The authors acknowledge the support of the latter, which is partially funded by the European Regional Development Fund (ERDF) via the Welsh Government. Yan-Ying Wu thanks the financial support from the School of Chemistry at Cardiff University and the U.K. Engineering and Physical Sciences Research Council (EPSRC) through Grant EP/W03431X/1.

■ REFERENCES

(1) (a) Solà, M. Aromaticity rules. *Nat. Chem.* **2022**, *14*, 585−590. (b) Savarese, M.; Brémond, É.; Ciofini, I.; Adamo, C. Electron Spin Densities and Density Functional Approximations: Open-Shell Polycyclic Aromatic Hydrocarbons as Case Study. *J. Chem. Theory Comput.* **2020**, *16*, 3567−3577. (c) Bhat, V.; Callaway, C. P.; Risko, C. Computational Approaches for Organic Semiconductors: From Chemical and Physical Understanding to Predicting New Materials. *Chem. Rev.* **2023**, *123*, 7498−7547.

(2) (a) Liu, Z.; Fu, S.; Liu, X.; Narita, A.; Samori, P.; Bonn, M.; Wang, H. I. Small Size, Big Impact: Recent Progress in Bottom-Up Synthesized Nanographenes for Optoelectronic and Energy Applications. *Adv. Sci.* **2022**, *9*, 2106055. (b) Goyal, H.; Kumar, P.; Gupta, R. Polycyclic Aromatic Hydrocarbon-Based Soft Materials: Applications in Fluorescent Detection, Gelation, AIEE and Mechanochromism. *Chem. - Asian J.* **2023**, *18*, No. e202300355. (c) Wang, Y.; Liu, B.; Koh, C. W.; Zhou, X.; Sun, H.; Yu, J.; Yang, K.; Wang, H.; Liao, Q.; Woo, H. Y.; Guo, X. Facile Synthesis of Polycyclic Aromatic Hydrocarbon (PAH)-Based Acceptors with Fine-Tuned Optoelectronic Properties: Toward Efficient Additive-Free Nonfullerene Organic Solar Cells. *Adv. Energy Mater.* **2019**, *9*, 1803976.

(3) (a) Parenti, K. R.; Chesler, R.; He, G.; Bhattacharyya, P.; Xiao, B.; Huang, H.; Malinowski, D.; Zhang, J.; Yin, X.; Shukla, A.; Mazumdar, S.; Sfeir, M.; Campos, L. M. Quantum Interference Effects Elucidate Triplet-Pair Formation Dynamics in Intramolecular Singlet-Fission Molecules. *Nat. Chem.* **2023**, *15*, 339−346. (b) Bae, Y. J.; Kang, G.; Malliakas, C. D.; Nelson, J. N.; Zhou, J.; Young, R. M.; Wu, Y.-L.; Van Duyne, R. P.; Schatz, G. C.; Wasielewski, M. R. Singlet Fission in 9,10-Bis(phenylethynyl)anthracene Thin Films. *J. Am. Chem. Soc.* **2018**, *140*, 15140−15144. (c) Margulies, E. A.; Wu, Y.-L.; Gawel, P.; Miller, S. A.; Shoer, L. E.; Schaller, R. D.; Diederich, F.; Wasielewski, M. R. Sub-Picosecond Singlet Exciton Fission in Cyano-Substituted Diaryltetracenes. *Angew. Chem., Int. Ed.* **2015**, *54*, 8679−8683.

(4) Zhang, L.; Cao, Y.; Colella, N. S.; Liang, Y.; Brédas, J.-L.; Houk, K. N.; Briseno, A. L. Unconventional, Chemically Stable, and Soluble Two-Dimensional Angular Polycyclic Aromatic Hydrocarbons: From Molecular Design to Device Applications. *Acc. Chem. Res.* **2015**, *48*, 500−509.

(5) (a) Zhang, L.; Fonari, A.; Liu, Y.; Hoyt, A.-L. M.; Lee, H.; Granger, D.; Parkin, S.; Russell, T. P.; Anthony, J. E.; Brédas, J.-L.; Coropceanu, V.; Briseno, A. L. Bistetracene: An Air-Stable, High-Mobility Organic Semiconductor with Extended Conjugation. *J. Am. Chem. Soc.* **2014**, *136*, 9248−9251. (b) Wang, Z.; Li, R.; Chen, Y.; Tan, Y.-Z.; Tu, Z.; Gao, X. J.; Dong, H.; Yi, Y.; Zhang, Y.; Hu, W.; Müllen, K.; Chen, L. A Novel Angularly Fused Bistetracene: Facile Synthesis, Crystal Packing and Single-Crystal Field Effect Transistors. *J. Nater. Chem. C* **2017**, *5*, 1308−1312.

(6) (a) Zhao, W.-L.; Li, M.; Lu, H.-Y.; Chen, C.-F. Advances in Helicene Derivatives with Circularly Polarized Luminescence. *Chem. Commun.* **2019**, *55*, 13793−13803. (b) Mori, T. Chiroptical Properties of Symmetric Double, Triple, and Multiple Helicenes. *Chem. Rev.* **2021**, *121*, 2373−2412. (c) Kiran, V.; Mathew, S. P.; Cohen, S. R.; Hernández Delgado, I.; Lacour, J.; Naaman, R. Helicenes—A New Class of Organic Spin Filter. *Adv. Mater.* **2016**, *28*, 1957−1962.

(7) (a) Liu, J.; Feng, X. Synthetic Tailoring of Graphene Nanostructures with Zigzag-Edged Topologies: Progress and Perspectives. *Angew. Chem., Int. Ed.* **2020**, *59*, 23386−23401. (b) Mishra, S.; Beyer, D.; Eimre, K.; Kezilebieke, S.; Berger, R.; Gröning, O.; Pignedoli, C. A.; Müllen, K.; Liljeroth, P.; Ruffieux, P.; Feng, X.; Fasel, R. Topological Frustration Induces Unconventional Magnetism in a Nanographene. *Nat. Nanotechnol.* **2020**, *15*, 22−28.

(8) Chan, J. M. W.; Tischler, J. R.; Kooi, S. E.; Bulović, V.; Swager, T. M. Synthesis of *J*-Aggregating Dibenz[*a*, *j*]anthracene-Based Macrocycles. *J. Am. Chem. Soc.* **2009**, *131*, 5659−5666.

(9) Zimmerman, S. C.; Zeng, Z.; Wu, W.; Reichert, D. E. Synthesis and Structure of Molecular Tweezers Containing Active Site Functionality. *J. Am. Chem. Soc.* **1991**, *113*, 183−196.

(10) (a) Ruffieux, P.; Wang, S.; Yang, B.; Sánchez-Sánchez, C.; Liu, J.; Dienel, T.; Talirz, L.; Shinde, P.; Pignedoli, C. A.; Passerone, D.; Dumslaff, T.; Feng, X.; Müllen, K.; Fasel, R. On-Surface Synthesis of Graphene Nanoribbons with Zigzag Edge Topology. *Nature.* **2016**, *531*, 489−492. (b) Yang, B.; Gu, Y.; Paternò, G. M.; Teyssandier, J.; Maghsoumi, A.; Barker, A. J.; Mali, K. S.; Scotognella, F.; De Feyter, S.; Tommasini, M.; Feng, X.; Narita, A.; Müllen, K. Zigzag-Edged Polycyclic Aromatic Hydrocarbons from Benzo[*m*]tetraphene Precursors. *Chem. - Eur. J.* **2023**, *29*, No. e202203981.

(11) Miyoshi, H.; Nobusue, S.; Shimizu, A.; Tobe, Y. Non-Alternant Non-Benzenoid Kekulenes: The Birth of a New Kekulene Family. *Chem. Soc. Rev.* **2015**, *44*, 6560−6577.

(12) (a) Diederich, F.; Schneider, K.; Staab, H. A. Dibenz[*a*, *j*]anthracene via Photo-Cyclodehydrogenation of 9,10-Dihydro-2-styrylphenanthrene. *Chem. Ber.* **1984**, *117*, 1255−1258. (b) Studt, P. Notizüber die Synthese von Dibenz[*a*, *j*]anthracen. *Justus Liebigs Annalen der Chemie* **1978**, *1978*, 2105−2106. (c) Noller, K.; Kosteyn, F.; Meier, H. Photochemie Elektronenreicher 1,3-Distyrylbenzole. *Chem. Ber.* **1988**, *121*, 1609−1615.

(13) (a) Pollart, D. J.; Rickborn, B. Cycloadducts of Arynes with 1,3-Bis(trimethylsilyl)naphtho[1,2-c]furan: Formation of Novel Polycyclic Aromatic Derivatives and Related Reactions. *J. Org. Chem.* **1986**, *51*, 3155−3161. (b) Pozo, I.; Majzik, Z.; Pavliček, N.; Melle-Franco, M.; Guitián, E.; Peña, D.; Gross, L.; Pérez, D. Revisiting Kekulene: Synthesis and Single-Molecule Imaging. *J. Am. Chem. Soc.* **2019**, *141*, 15488−15493.

(14) (a) Bonifacio, M. C.; Robertson, C. R.; Jung, J.-Y.; King, B. T. Polycyclic Aromatic Hydrocarbons by Ring-Closing Metathesis. *J. Org. Chem.* **2005**, *70*, 8522−8526. (b) Nakakuki, Y.; Hirose, T.; Matsuda, K. Synthesis of a Helical Analogue of Kekulene: A Flexible π-Expanded Helicene with Large Helical Diameter Acting as a Soft Molecular Spring. *J. Am. Chem. Soc.* **2018**, *140*, 15461−15469.

(15) (a) Chen, Q.; Brambilla, L.; Daukiya, L.; Mali, K. S.; De Feyter, S.; Tommasini, M.; Müllen, K.; Narita, A. Synthesis of Triply Fused Porphyrin-Nanographene Conjugates. *Angew. Chem., Int. Ed.* **2018**, *57*, 11233−11237. (b) Qiang, P.; Sun, Z.; Wan, M.; Wang, X.; Thiruvengadam, P.; Bingi, C.; Wei, W.; Zhu, W.; Wu, D.; Zhang, F.

Successive Annulation to Fully Zigzag-Edged Polycyclic Heteroaromatic Hydrocarbons with Strong Blue−Green Electroluminescence. *Org. Lett.* **2019**, *21*, 4575−4579. (c) Opie, C. R.; Noda, H.; Shibasaki, M.; Kumagai, N. Less Is More: $N(BOH)_2$ Configuration Exhibits Higher Reactivity than the B_3NO_2 Heterocycle in Catalytic Dehydrative Amide Formation. *Org. Lett.* **2023**, *25*, 694−697.

(16) (a) Tsai, H.-C.; Huang, Y.-H.; Chou, C.-M. Rapid Access to *Ortho*-Alkylated Vinylarenes from Aromatic Acids by Dearomatization and Tandem Decarboxylative C−H Olefination/Rearomatization. *Org. Lett.* **2018**, *20*, 1328−1332. (b) Wang, Y.-C.; Huang, Y.-H.; Tsai, H.-C.; Basha, R. S.; Chou, C.-M. Palladium-Catalyzed Proaromatic C(Alkenyl)−H Olefination: Synthesis of Densely Functionalized 1,3-Dienes. *Org. Lett.* **2020**, *22*, 6765−6770. (c) Tsai, J.-J.; Huang, Y.-H.; Chou, C.-M. Carboxylate-Assisted Palladium-Catalyzed Regio- and Stereoselective Mizoroki−Heck Arylation of *β*-Cyclohexadienyl Acrylates and Styrenes. *Org. Lett.* **2021**, *23*, 9468−9473.

(17) (a) Liu, Z.; Larock, R. C. Facile *O*-Arylation of Phenols and Carboxylic Acids. *Org. Lett.* **2004**, *6*, 99−102. (b) Wen, C.; Chen, Q.; He, Z.; Yan, X.; Zhang, C.; Du, Z.; Zhang, K. The Insertion of Arynes into the O−H Bond of Aliphatic Carboxylic Acids. *Tetrahedron. Lett.* **2015**, *56*, 5470−5473.

(18) Trost, B. M. Dehydrogenation Mechanisms. On the Mechanism of Dehydrogenation of Acenaphthene by Quinones. *J. Am. Chem. Soc.* **1967**, *89*, 1847−1851.

(19) Zimmerman, S. C.; Wilson, S. R. Structures of Methyl 7-Phenyldibenz[*a*, *j*]anthracene-14-carboxylate and Methyl 7-Phenylbenzo[1,2-*h*:5,4-*h*′]diquinoline-14-carboxylate: Twisted Aromatic Spacers Containing Bay-Region Esters. *Acta Crystallogr.* **1992**, *C48*, 703−706.

(20) Clar, E. *The Aromatic Sextet*; John Wiley and Sons: London, U.K., 1972.

(21) (a) Dewar, M. J. S.; Longuet-Higgins, H. C. The Electronic Spectra of Aromatic Molecules I: Benzenoid Hydrocarbons. *Proc. Phys. Soc. A* **1954**, *67*, 795−804. (b) Moffitt, W. Configurational Interaction in Simple Molecular Orbital Theory. *J. Chem. Phys.* **1954**, *22*, 1820−1829.

https://doi.org/10.1021/acs.orglett.3c02306
Org. Lett. XXXX, XXX, XXX−XXX